

Chapter 1

Introduction

The work presented in this thesis explores the possibilities of using laser speckle field in various imaging modalities for industrial and biomedical applications. The motivation behind the work was to develop and design simple and low-cost optical arrangements for (1) measurement of various optical (optical rotation and refractive index) and physical properties (temperature and magnetic field) (2) mapping time-varying refractive index profiles to study heat diffusion in dielectric slab and using this information to locate abnormalities such as defect (3) quantitative phase contrast imaging of Red blood cells (4) shape measurement of asymmetric objects. The basic and common element in all these applications is laser speckles which aided in accomplishing these objectives of the thesis. The simplistic and ergonomic nature of one of the developed system (for measurement of refractive index) has encouraged designing a stand-alone device using 3D printing technology.

1.1 The Speckle Phenomenon

With the commercial availability of continuous-wave lasers in the 1960s, many researchers and engineers working with it had noticed a strange phenomenon. It was observed that when the laser light was reflected from a rough surface like that of a paper or the wall of the laboratory, a high-contrast fine-scale granular pattern would appear near the scattering spot [1]. Even though the laser-produced beam of light was intense, collimated, narrow, monochromatic and coherent, the images by its illumination were contaminated by the grainy structures which limited the effective resolution. Thus, many researchers have developed various means (optical and numerical) to tackle this problem [2–8]. This granularity was random intensity distributions in space and was generated despite the fact that the illumination spot was relatively uniform. This granular structure is known as laser speckles. Soon after the discovery of laser speckles, it was noticed that the speckle pattern could carry information and thus, efforts were made towards harnessing the potential of laser speckle and employ it for metrology applications [9–11]. After the discovery

of laser speckle and realization of its potential, it is considered as a versatile tool in numerous applications. Techniques such as speckle interferometry, speckle photography, laser speckle contrast imaging, speckle correlation [1,10,12–14] have been developed.

When an optically rough surface is illuminated with light having a high degree of coherence, the intensity of the scattered light is distributed randomly to cover the surrounding space with a fine granular structure consisting of randomly distributed alternately dark and bright spot of variable shapes that has no relation with the macroscopic properties of the surface. This random intensity distribution is also observed when coherent light propagated through a medium due to the random variations in its refractive index. Such intensity distribution is known as a speckle pattern [14]. The laser speckle pattern is formed due to the interference of the de-phased wavelets (due to reflection from an optically rough surface or by propagation through a medium of random refractive index) which originates from the same coherent source resulting in random interference pattern which is known as speckles. In other words, the laser speckle pattern is the resultant intensity generated by the interference of randomly phased elementary contributions resulting from various microscopic facets of the rough scattering medium. The resultant intensity may be weak or strong depending on the particular set of random phases present. A diffuser has a surface with random surface variations and thus, creates spatially changing random angles of incidences for the laser beam and thus, the optical path of different light rays passing through the transmissive object vary significantly in length on a scale of wavelength of visible light thereby creating laser speckles [1]. A sample of the laser speckle pattern is shown in Fig. 1.1. It is also reported in works of literature that the dark and bright spots in the speckle pattern occur with different frequencies and the dark spots are much more common than the bright ones [10,15].

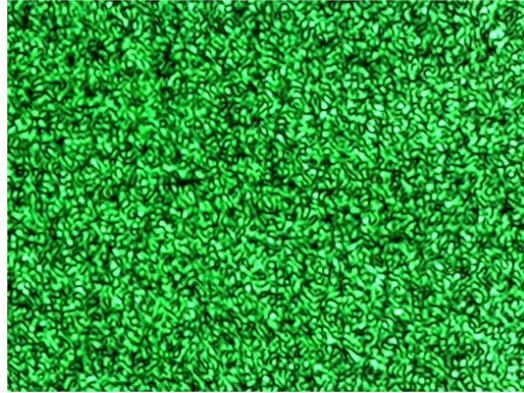


Fig 1. 1: A laser speckle pattern

1.2 Types of Laser Speckle

Since the laser speckle patterns fill the space surrounding the medium generating it, to observe a speckle pattern there is no compulsion to use an image forming system. The speckle pattern observed from the free propagation is known as objective speckle pattern while the speckle pattern observed using an imaging system is known as subjective speckle pattern [14]. Fig. 1.2 describes the arrangements for obtaining an objective speckle pattern (free space geometry) and subjective speckle pattern (imaging system).

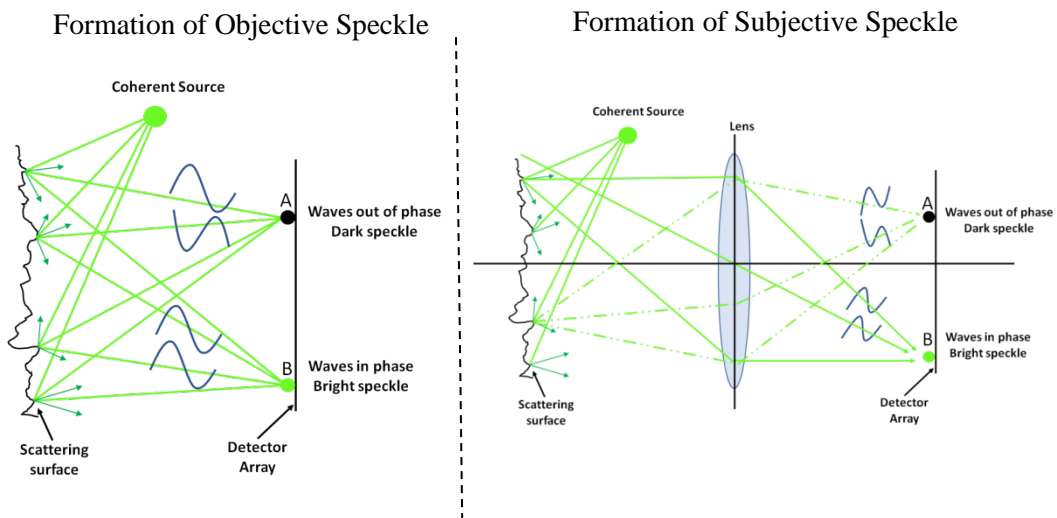


Fig 1. 2: Geometries for the formation of objective and subjective speckle

1.3 Contrast of Laser Speckle

Now, the important fact is that every point on the screen receives light waves that are scattered from every point of the illuminated object. Thus, there will be a multitude of scattered waves coming to any single point of the screen. Furthermore, these converging scattered waves have traveled different path lengths, and they arrive with a multitude of different phases. They interfere with one another to produce a particular brightness at the meeting point. Thus, the light field at a specific point $P(x, y, z)$ in a speckle pattern must be the sum of a large number N of components representing the contribution from all points on the scattering surface. Let an optically rough surface be illuminated by a polarized monochromatic light, the contribution to the field at point P produced by any surface element j is given [5]

$$u_j(P) = |u_j| e^{i\phi_j} = |u_j| e^{ikr_j} \quad (1.1)$$

where r_j is the randomly varying distance from the j th scattering surface element to the point P .

The complex amplitude of the scattered field at point P can be written as

$$U(P) = \frac{1}{\sqrt{N}} \sum_{j=1}^N u_j(P) = \frac{1}{\sqrt{N}} \sum_{j=1}^N |u_j| e^{i\phi_j} = \frac{1}{\sqrt{N}} \sum_{j=1}^N |u_j| e^{ikr_j} \quad (1.2)$$

The summation described in Eq. (1.2) can be considered as a random walk in the complex plane due to the random phases $\phi_j = kr_j$ which is represented in Fig. 1.3 as an erratic motion of the field components.

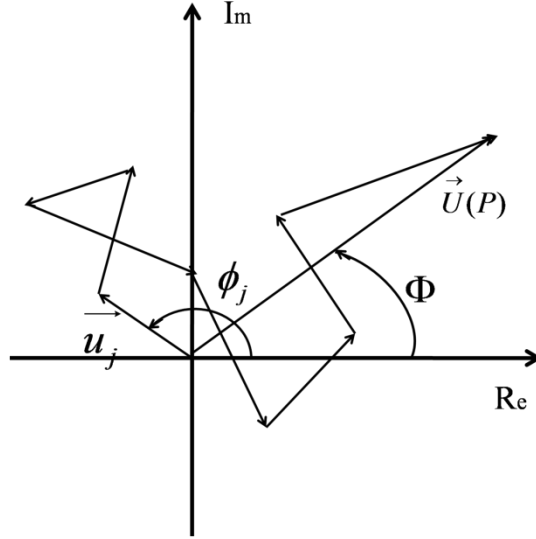


Fig 1. 3: Several scattered fields $u_j(P)$, plotted in the complex plane with their respective random phases, contributing to the total field at point P , $U(P)$

Before proceeding further, some assumptions need to be considered; (1) the amplitude u_j and phase ϕ_j of each field component are statistically independent of each other and are also independent of the amplitude and phase of all other field components and (2) the phases ϕ_j are uniformly distributed on the interval $(-\pi, \pi)$ which means that the surface is rough in comparison to the wavelength, and with the additional hypothesis that the number of total scattering centers N is very large, thus ensuring validity of the central limit theorem.

It was demonstrated by Goodman that real and imaginary parts of the resultant field are asymptotically Gaussian[1,2]. The joint probability density function of them is given by [6]

$$p_{r,i}(U^{(r)}, U^{(i)}) = \frac{1}{2\pi\sigma^2} \exp\left[-\frac{(U^{(r)})^2 + (U^{(i)})^2}{2\sigma^2}\right] \quad (1.3)$$

Known as circular Gaussian where

$$\sigma^2 = \lim_{N \rightarrow \infty} \sum_{j=1}^N \frac{\langle |u_j|^2 \rangle}{2} \quad (1.4)$$

From Equation 1.3, and taking into account that the intensity I and phase Φ of the resultant field are related to the real and imaginary parts of the field according to

$$\begin{aligned} U^{(r)} &= \sqrt{I} \cos \Phi \\ U^{(i)} &= \sqrt{I} \sin \Phi \end{aligned} \quad (1.5)$$

it follows that the probability density of the intensity $p(I)$ and of the phase $p(\Phi)$ are given by

$$p(I) = \frac{1}{\langle I \rangle} e^{-\frac{I}{\langle I \rangle}} \quad \text{for } I \geq 0 \quad (1.6)$$

$$p(\Phi) = \frac{1}{2\pi} \quad \text{for } -\pi \leq \Phi \leq \pi \quad (1.7)$$

respectively. In Eq.(1.6), $\langle I \rangle$ stands for the mean value of the intensity in the speckle diagram. Thus, according to Eq. (1.6) and Eq. (1.7), the intensity distribution follows a negative exponential law, whereas the phase is uniformly distributed in the interval $(-\pi, \pi)$. The probability density function of Eq. (1.6) is illustrated in Fig. 1.4.

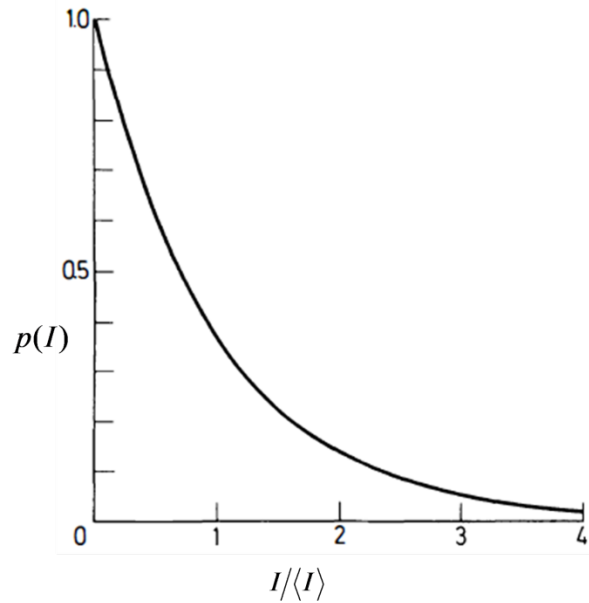


Fig 1. 4: Normalized probability density function and probability that the intensity exceeds level for a polarized speckle pattern

The moments of intensity distribution are defined as [5]

$$\langle I^n \rangle = n!(2\sigma^2)^n = n!\langle I \rangle^n \quad (1.8)$$

and of special interest are the second-order moment and the variance:

$$\langle I^2 \rangle = 2\langle I \rangle^2 \text{ and } \sigma_1^2 = \langle I^2 \rangle - \langle I \rangle^2 = \langle I \rangle^2 \quad (1.9)$$

Eq. (1.9) shows, that the standard deviation of a polarized speckle pattern equals the mean value of the intensity. A usual measure of the degree of modulation of a speckle pattern is called *the contrast*, defined as

$$C = \frac{\sigma_1}{\langle I \rangle} \quad (1.10)$$

This definition (Eq. (1.10)), together with the result in Eq.(1.9), means that the contrast of a polarized speckle pattern is always unity, and the speckle pattern is said to be fully developed

1.4 Lateral and Axial size of Laser Speckles

Since laser speckle is a random phenomenon, it becomes essential to understand and analyze it statistically. One such statistical property is the average size of the speckle which can be considered as a measure of the extent of the spatial correlation of the pattern and any point beyond that are considered as practically uncorrelated. The size (lateral size) of the objective speckles (ρ_o) forming at a distance d from the scattering surface (for free-space geometry) to the recording plane, D is the size of the illuminated spot and λ is the incident wavelength is given by [3].

$$\rho_o \approx \frac{\lambda d}{D} \quad (1.11)$$

For subjective speckle, the size of the speckle pattern can be computed by replacing D with D_{ap} (the aperture size of the lens) in Eq. 1.1 The axial size of the speckle (which looks similar to a cigar) is given by[4]

$$\Delta_{axial} = 8\lambda(d/D)^2 \quad (1.12)$$

where, d is the distance from the scattering surface (for free-space geometry) to the recording modality, D is the size of the illuminated spot, and λ is the incident wavelength.

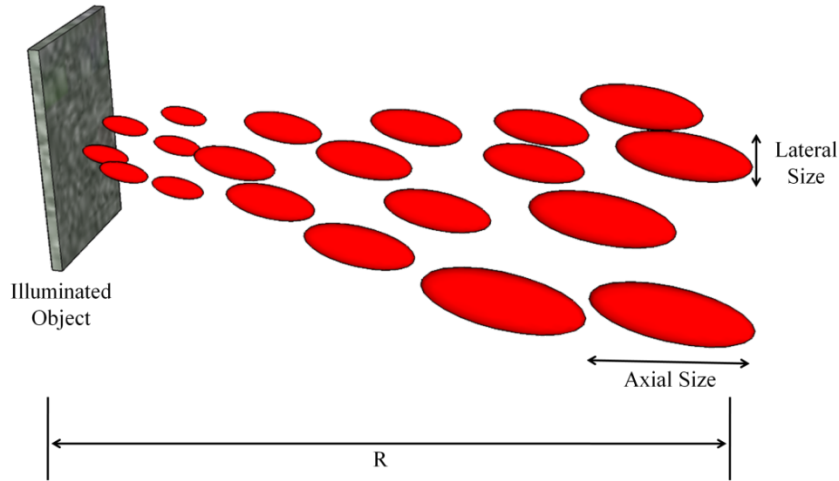


Fig 1. 5: Schematic showing axial and lateral speckle size

Fig. 1.5 represents the three-dimensional structure of the laser speckle generated from a rough surface either on reflection or transmission through it.

1.5 Laser Speckle in Optical Metrology

Owing to the mechanics of the formation of laser speckle, where the random phase differences from the scattering facets interfere, to observe a stable and static speckle pattern, the phase difference should remain constant (in space and with time). This leads to one of the advantages that the laser speckles offer; the ability to sense small changes in path length of various microscopic scattering facets. Therefore, if the rough surface generating the laser speckles gets into a motion, the phases, as well as the object-region contributing to generation of speckle, change with time, which may lead to a modulation in the speckle pattern. This establishes speckle pattern as a random carrier of information and can be employed to quantify translations, rotations, phase changes, etc. for a rough surface of translucent material and set the basis for a research field in the coherent optics named as Speckle Metrology [5].

In astronomy, speckle based techniques have been used to go beyond the resolution limit set by the atmospheric turbulence and able to achieve the diffraction limit of telescopes by short time exposure, which leads to a smaller speckle size and higher resolution [6]. The technique of Speckle Photography was introduced by Archbold *et al.*[7,8] and explored by Duffy [9], where the object under study is illuminated by a divergent, coherent beam from an angle and imaged by a camera. Two speckle patterns of the specimen before and after the deformation are recorded, where a fringe pattern depicting in-plane displacement due to the deformation can be extracted from the processed photographic film using a Fourier filtering technique. So, if the speckle pattern remains the same between the two exposures both the recorded patterns are fully correlated over the entire area of the registered medium, thus maximizing the visibility of the resulting fringes[10]. Speckle interferometry is also one of the approaches in the field of speckle metrology which was first proposed by Leendertz at the beginning of 1970 [5]. The desired information is codified in the correlation fluctuations of the involved speckle pattern. The development of better processing and recording modalities such as digital cameras and frame grabbers capable of many built-in operations has encouraged the appearance of the first opto-digital devices leading to a technique known today as electronic speckle pattern interferometry (ESPI) or TV holography [5].

There are cases when the laser light gives rise to the speckle pattern where the laser light interacts with objects that shows some kind of activity (fruit, paints in process of drying, or some kind of biological samples), the visual appearance of the patterns resembles a boiling liquid. Such an effect is known as dynamic speckle and it is a result of the movements of the scattering centers (variations in the phase of the light) owing to changes in the refractive index, optical rotation, etc.[5]. This effect can be used to study the time varying properties of the medium under investigation.

1.6 Outline of the thesis

The work described in the thesis focuses on providing simple and cost-effective solutions for metrology and imaging applications using the laser speckle field.

Chapter 1 provides an introduction and overview of the laser speckle and some of its properties. It provides a brief of the techniques involved in the work and the detailed discussion and introduction to each technique is covered in their respective chapters.

Chapter 2 introduces the speckle correlation technique and discusses various correlation algorithms. It also provides the flow chart of the algorithm which will be used in Chapter 3 and Chapter 4.

Chapter 3 describes the use of a speckle correlation technique for the measurement of optical properties like optical rotation and refractive index. Faraday effect and optical activity are discussed for understanding optical rotation and a 3D printed refractometer is designed and developed.

Chapter 4 discusses the use of speckle correlation technique for measurement of physical properties such as temperature and magnetic field. For the measurement purpose, a cantilever action of a metal strip is used to sense the change in the measuring quantity and this change is converted into a change in correlation coefficient values for calibrating the system.

Objective speckle pattern is used with the correlation technique to measure optical rotation, refractive index, temperature and magnetic field (Chapter 3 and Chapter 4). Sensing change in the measured quantity by quantifying the change in speckle pattern for two different levels of the measured quantity serves the basis of Chapter 3 and Chapter 4.

Chapter 5 explains the use of a single beam lensless Fourier transform digital holography together with speckle field for macroscopic and microscopic applications. The macroscopic application includes studying of conduction of heat by mapping refractive index distributions and using it for defect detection while the

microscopic application includes the quantitative phase contrast microscopy for imaging RBCs. Objective speckle pattern generated by a ground glass diffuser together with the principles of lensless Fourier transform digital holography utilizes the properties of speckle field that the information from every microscopic scattering facets reaches the recording medium thereby allowing more information to be collected by the recording device and hence increasing the resolution.

Chapter 6 describes the application of iterative phase retrieval technique together with the speckle field for shape measurement by two-wavelength contouring. Speckle field was used to incur a significant change in the recorded intensity at each sampling plane thereby enhancing the quality and the rate of convergence in the iterative phase retrieval technique.

Chapter 7 concludes the outcomes of the thesis and discusses the future prospects of utilizing speckle fields for biomedical applications.